

EFFECTS OF DESIGN AND OPERATING PARAMETERS OF FILTERED VENTING ON CONTAINMENT DEPRESSURIZATION AND FISSION PRODUCT RELEASE

Jong Woon Park, Wook-Cheol Seol, Jisu Kim

Dongguk University, 123 Dongdae-ro, Gyeongju, Gyeongbuk, 38066, Republic of Korea, jwoonp@gmail.com

Effects of design and operational parameters of filtered containment venting system on a specified containment depressurization and relative aerosol release amount are analyzed. The parameters considered are piping size and discharge coefficient of the vent line, vent initiation pressure, and stroke time of the isolation valves between the containment and the venting system. The analyses are performed by using the MAAP4 code for the APRI400 reactor with rated thermal power of 4,000 MW. The containment is divided into 12 control volumes and the two-phase single volume of the venting system node is added to the containment upper compartment with a junction. The venting system is modeled using a stratified two-phase volume accommodating steam and non-condensable gas effluent from the containment. The decontamination factor for CsI aerosol is conservatively assumed to be 100, only considering minimum pool scrubbing performance under degraded FCVS condition. Major results uniquely identified from the analyses can be noted as following: Even though containment depressurization is accelerated as the pipe size increases, the venting system solution is also depleted earlier. Elapsed times to reach lower end pressure of 2 bar are nearly identical regardless of the vent initiation pressure and thus early venting is not much beneficial than late venting. Stroke time of the isolation valves has no effect on the depressurization performance and thus slow opening is beneficial for load reduction from the vent effluent. One thing to be noted about CsI release standpoint, the released mass for the low pressure venting may be larger than for the uncontrolled failure at much higher pressure when the decontamination factor is low. It is found that this is because, when we vent at lower containment pressure, in-containment gas contains less steam than at higher containment pressure and the CsI concentration of the effluent from the containment tends to increase.

I. INTRODUCTION

Filtered Containment Vent Systems (FCVSs) have been installed in European nuclear plants for controlled depressurization of a containment under severe accident. This is to keep the containment from overpressure or the large amount of radioactive gas-steam mixture from the containment may discharge into environment. Although containment depressurization as a primary objective of the FCVS is successful, the decontamination feature could fail by the continuous evaporation of the scrubbing solution after long operation. During the operation, the atmosphere of the FCVS becomes slightly above the saturation temperature owing to the release of high temperature steam and heat releasing aerosols. The important issues of designing and operating the systems are mainly two-folded: one is the depressurization capacity and the other is aerosol removal capacity.

We can provide several previous studies on this matter. Lee et al. (Ref. 1) studied depressurization characteristics of the OPR1000 plant under station blackout (SBO) and loss of coolant accidents. They treated this matter simply by using a junction and isolation valves without a FCVS model. They considered cyclic operation of the FCVS and demonstrated the advantage of containment depressurization using a vent line. However, their model has a limitation in that it does not consider the FCVS tank solution and thus they didn't address about the FCVS behavior itself.

Yuan et al. (Ref. 2) performed containment venting strategy analysis via a containment air filtration system using integral safety analysis code for a large break loss of coolant accident. They considered effects of two pipe sizes and several vent initiation pressures. The effect of venting pipe size shows the advantage of depressurization and mitigation of overpressure failure. Venting open pressure affected released aerosol mass. The aerosols mass released decreases when venting starts at higher pressure. However, they only modeled the venting pipes, not the FCVS itself.

On the other hand, Na et al. (Ref. 3) studied the thermal hydraulic issues in the FCVS for a long operating time using the MELCOR computer code. The modeling of the FCVS, including the models for pool scrubbing and the filter, was added in the OPR-1000 containment model. SBO was chosen as an accident scenario and the effect of FCVS inlet and outlet pipe sizes was considered. The effect of outlet piping size is much greater than that of the inlet piping and this is because the discharge resistance of gases in the FCVS increases with the decrement of the exhaust pipe size.

Dejardin et al. (Ref. 4) suggested key design parameters and they are pressure range, venting flow, stored decay energy, stored aerosol mass and decontamination factor. They used fixed design values of as-built Belgian plant and they did not consider variable design and operating parameters. One thing to be noted is that safe flow rate through a venting pipe is determined to be 5 kg/s. However, this value cannot be generalized.

USNRC (Ref. 5) studied hardened venting for a BWR using MELCOR code for diverse options of operations. They assumed pool decontamination factor of 500. An intensive survey by OECD/NEA (Ref. 6) provides similar FCVS parameters: vent initiation, vent flow rate capacity, thermal load, aerosol load and characteristics, iodine load, autonomous time for unattended FCVS operation and hydrogen load which affect containment depressurization and decontamination factor.

The literature survey above shows that there have been limited modeling and analyses regarding separate and integral effects of diverse design and operating parameters of the FCVS on the containment depressurization and aerosol release. This motivates the present study seeking to investigate those separate and integral effects after selecting common key parameters. The parameters selected are venting pipe size, discharge coefficient, vent initiation pressure, stroke time, which affect flow rate and consequently the depressurization rate and CsI release mass. This would cover almost all the key design parameters suggested by Dejardin et al. (Ref. 4) and OECD/NEA (Ref. 6). APR1400, which is a 4,000 MWt evolutionary nuclear power plant, is selected as the target plant for the present analysis. The scenario considered is a SBO with concurrent failure of emergency feed water pumps. The code used is the severe accident analysis code MAAP4. The containment is divided into 12 control volumes and the stratified gas-liquid volume of the venting system node is connected to the containment upper compartment with a junction. A venturi scrubber (VS), which is used in the FCVS for enhancing scrubbing of aerosols, is not considered but only the FCVS water pool scrubbing effect is considered by conservatively assuming constant pool decontamination factor (DF) of 100 presuming degraded condition of the FCVS. Also, metallic filter that is installed before the exit piping is not considered.

II. METHOD OF ANALYSIS

II.A. Models for Containment and Filtered Containment Venting System

The containment for the APR1400 is divided into 12 control volumes and they are interconnected by 41 junctions as shown in Fig. 1. Before describing the thermal-hydraulic model of FCVS, a water pool model for a wet type FCVS will be described here. As shown in Fig. 2, the wet type FCVS consists of two-phase water pool ($V_{2\phi}$), gas region (V_g) and inlet and outlet pipes. The inlet piping is submerged in liquid water at the bottom and the outlet piping is connected to the gas region.

The generic water pool model in the MAAP4 code (Ref. 7) is a single volume composed of lower two-phase mixture sub-volume and upper ideal gas sub-volume as shown in Fig. 2. The rate of volume change of the lower two-phase mixture can be described by:

$$\frac{dV_{2\phi}}{dt} = \dot{m}_w \cdot v_w + \dot{m}_s \cdot v_s + \dot{m}_{nc} \cdot v_{nc} - j_g \cdot A_p \quad (1)$$

where \dot{m}_w is the rate of water mass change in a pool, v_w the specific volume of water, \dot{m}_s the steaming rate in a pool, v_s the specific volume of saturation steam, \dot{m}_{nc} the incoming non-condensable (NC) gas flow rate, v_{nc} the specific volume of NC gas at the pool temperature and A_p the surface area of the two-phase mixture volume through which gas leaves.

The gas volume V_g as shown in Fig. 2 is obtained from the ideal gas law as following:

$$V_g(P_p) = \frac{P_{sat}}{P_p} V_g(T_p) \quad (2)$$

where P_p is the pressure at the pool surface and P_{sat} is the saturation pressure.

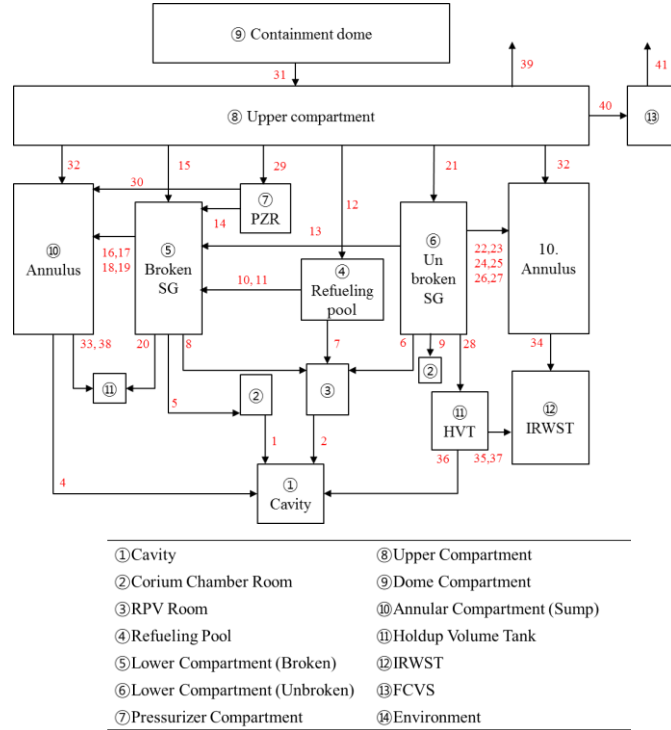


Fig. 1. Containment control volumes of APR 1400

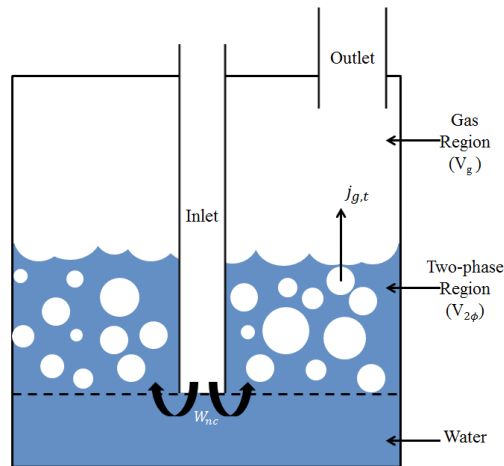


Fig. 2. Water pool model for FCVS.

The present FCVS control volume connected with the containment and environment is configured as in Fig. 3. The inlet piping runs from the containment volume node 8 shown in Fig. 1. The FCVS is a cylindrical tank with the height of 6.5 m, the diameter of 2 m, and the total volume of 18.84 m³. This dimension is set to be the same as the previous study using the MELCOR code (Ref. 3) so that we can potentially compare the major results. It is assumed that the lower part of the FCVS is water height of 3 m and the upper part is air. The states of the two isolation valves on the inlet and outlet junctions are modeled using the Bernoulli junction models (Ref. 7). The inlet junction is positioned at 1.5m from the FCVS bottom.

At the top of the tank, there practically is a metallic filter and multiple venturi scrubbers are generally attached to the end of the inlet piping to enhance the DF. However, this paper neglected the filtering effects of the two components by assuming constant value of DF of 100 due to pool scrubbing only and this value is conservatively low considering degraded FCVS conditions. The pressure drop along the metallic filter is not considered but the hydrodynamic and temperature effects of the venturi scrubbers are analyzed by varying discharge coefficients even though the value is as high as 0.98 (Ref. 8).

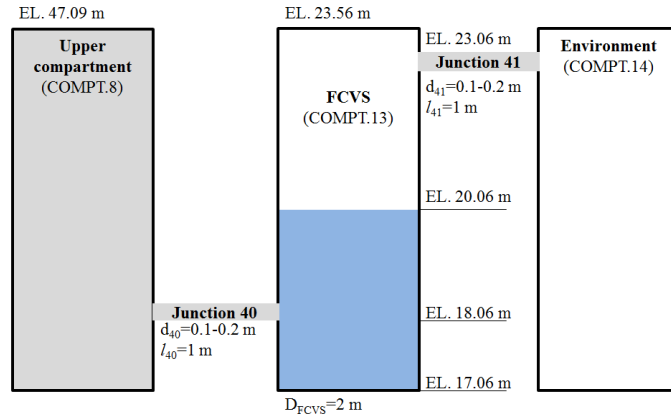


Fig. 3. Connections of FCVS with containment and environment

II.B. Analysis Parameters and Conditions

Selection of a typical accident scenario is necessary for the entire analyses hereinafter. The scenario selected is a station blackout with concurrent failure of emergency feed water pumps and subsequent opening of the two depressurization valves (POSRVs) at the core uncover (Ref. 9). The reactor vessel fails at approximately 40,000 sec and the containment fails at 325 hr (13.5 d) by assuming failure pressure of 1350 kPa as shown in Fig. 4(a) and 4(b), respectively.

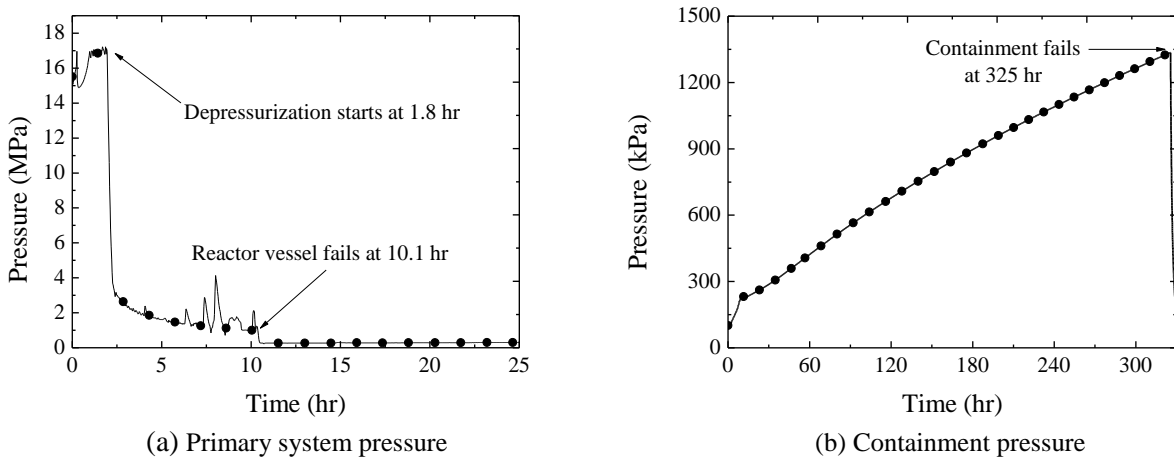


Fig. 4. Primary system and containment pressure variations for SBO

Analyses are conducted to investigate the influence of following design and operational parameters on the containment depressurization, FCVS behavior and CsI release:

- (1) Effect of pipe size
- (2) Effect of discharge coefficient
- (3) Effect of vent initiation pressure
- (4) Effect of stroke time
- (5) Fission product release to environment analysis

For the pipe size, the purpose is to investigate the influence on the containment depressurization effectiveness. Two sizes are considered, 10 cm and 20 cm of diameters. For the discharge coefficient, the purpose is the same as that of the pipe size, containment depressurization. Two values are used, 0.75 and 0.9. The maximum value of 0.9 used is slightly conservative because Silva et al. (Ref. 8) reported very large value of the discharge coefficient, 0.98, which means a negligible pressure loss. For the vent initiation pressure, two values, 4 and 7 bar, are used. For the stroke time, which means speed of valve opening, two times, 10 and 60 sec, are used. This would determine pipe loading which is very important for the discharge pipe design. As a reference case, uncontrolled containment failure at 8 bar with a break hole diameter of 20 cm without FCVS is also considered. TABLE 1 summarizes those analysis cases stated above as combinations of said parameters. Fission products, especially, the CsI aerosol release masses are compared between each case.

TABLE I. Analysis cases

Case ID	Containment pressure where vent initiates (bar)	Isolation valve stroke time (sec)	Pipe diameter (cm)	Decontamination factor CsI
P8D20FAIL	8	-	20	1
P4O10D10DF0	4	10	10	1
P4O10D10DF3	4	10	10	100
P7O10D10DF3	7	10	10	100
P4O10D20DF3	4	10	20	100
P4O60D10DF3	4	60	10	100

The results are organized into three sections: containment depressurization, FCVS water depletion and fission product release amount.

III. RESULTS AND DISCUSSION

III.A. Containment Depressurization

III.A.1 Effect of Pipe Size

The analysis results for the pipe size effects for the same vent initiation pressure of 4 bar are presented in terms of the containment pressure (node 8 in Fig. 1), the gas flow rate through the FCVS inlet junction (junction 40 in Figs. 1 and 3), the FCVS pressure and water temperature. They are shown in Fig. 5.

The analysis cases are P4O10D10DF0 and P4O10D10DF3 in TABLE I, where the pipe diameter are 10 cm and 20 cm, respectively and the isolation valves are opened at the same pressure of 4 bar. The time of vent initiation is 55 hr into the accident initiation as shown in Fig. 5(a). For the pipe diameter of 20 cm, it took 10 hrs to depressurize the containment to 2 bar and 78 hrs for the diameter of 10 cm. This result is naturally due to the difference of the discharge flow rates from the containment as shown in Fig. 5(b) where the maximum flow rate is 14.38 kg/s for the 20 cm pipe and 3.73 kg/sec for the 10 cm pipe. For the FCVS pressure shown in Fig. 5(c), 20 cm pipe case shows faster reduction of the pressure after peak and the water pool maximum temperature is lower as shown in Fig. 5(d). This is because the FCVS pressure follows the trend of a containment pressure and the pool saturation temperature is higher in higher pressure case. Therefore, it can be stated that for the same vent initiation pressure larger pipe is more useful for the containment depressurization and preserving lower pressure and temperature inside the FCVS.

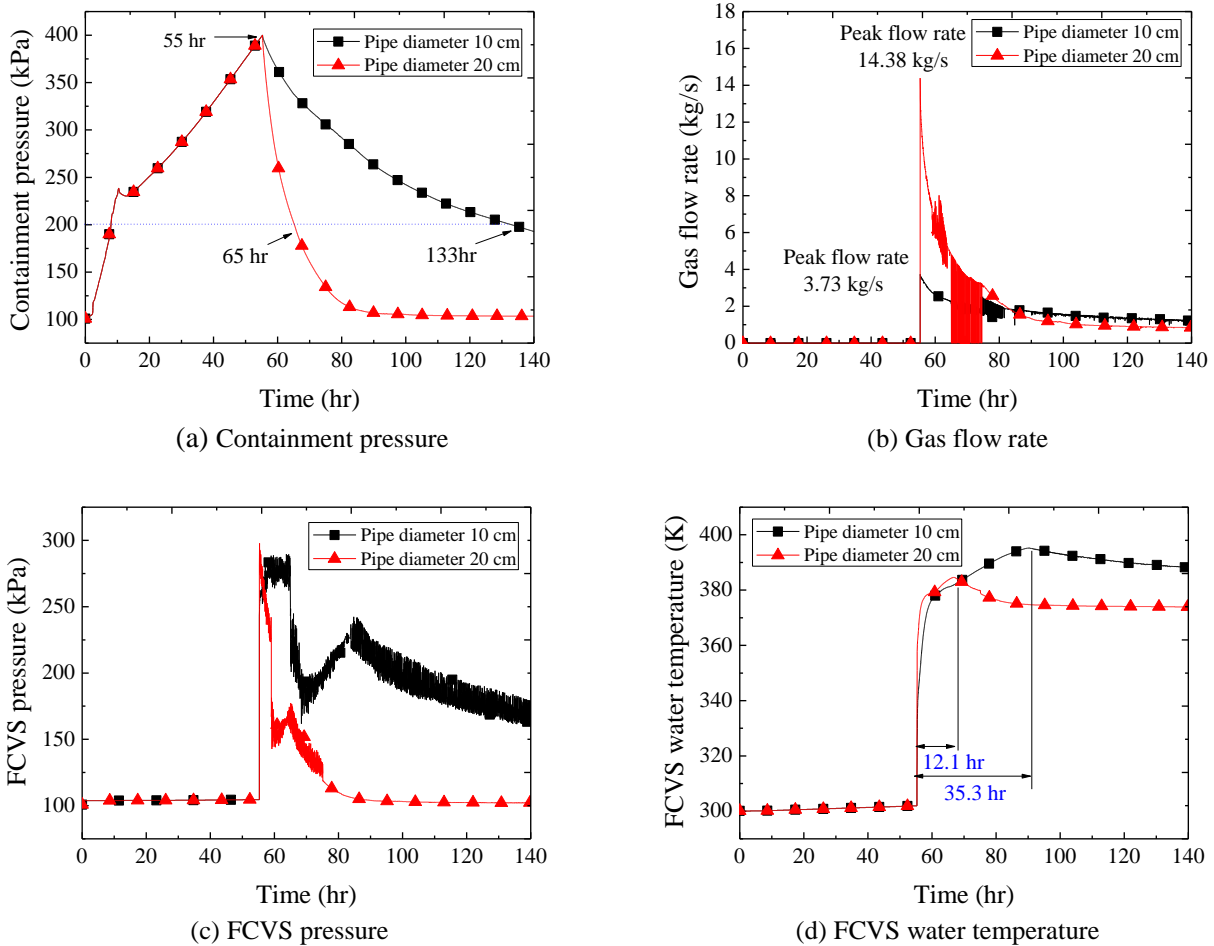


Fig. 5. Effect of pipe size.

III.A.2 Effect of FCVS Inlet Pipe Discharge Coefficient

This section describes the hydrodynamic and temperature effects of the discharge coefficient at the exit of the FCVS inlet piping on the containment and FCVS pressures and the FCVS water level. The case considered is P4O10D10DF3 where the vent initiation pressure is 4 bar and the pipe size is 10 cm.

Figure 6 shows the pressures of the containment and FCVS for two discharge coefficient values (C_d) of 0.75 and 0.9. The discharge coefficient of 0.75 is simulating partly blocked venturi scrubber. Nevertheless, the pressure differences are very small for these two discharge coefficients as shown in Fig. 6(a) and therefore it can be stated that there is no issue of not considering venturi scrubber in a hydrodynamic standpoint since the discharge coefficient of a typical venturi scrubber is about 0.98 which is very high so that it would not reduce the flow.

On the other hand, the difference of the evaporation rates of the FCVS water is significant as shown in Fig. 6(b) where the time elapsed between the vent initiation at 4 bar and the time of water level reaching minimum of 1.5 m (level of inlet piping) is reduced by about 4 hrs (from 16 hrs to 12 hrs) for the higher discharge coefficient of 0.9. This is the result of energy accumulation due to increased flow rate for the higher discharge coefficient.

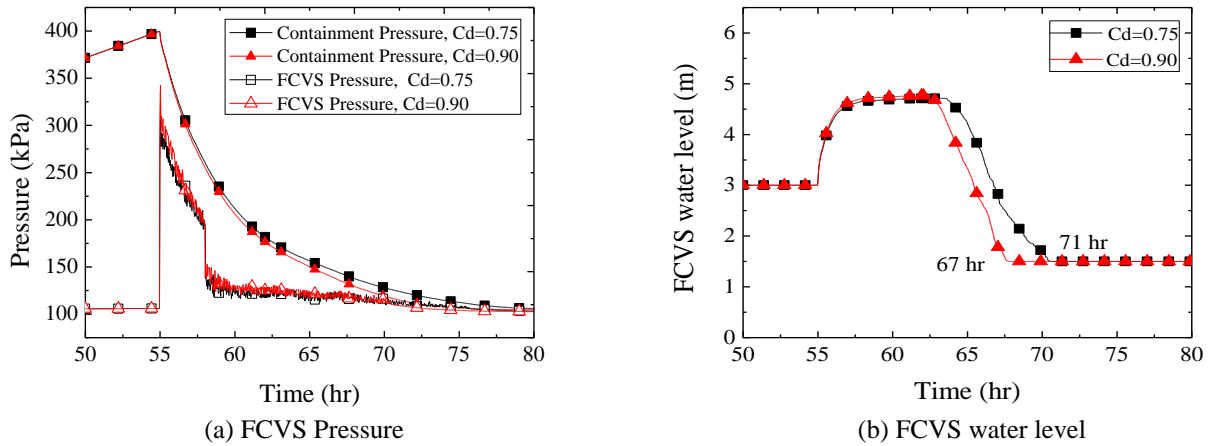


Fig. 6. Effect of discharge coefficient.

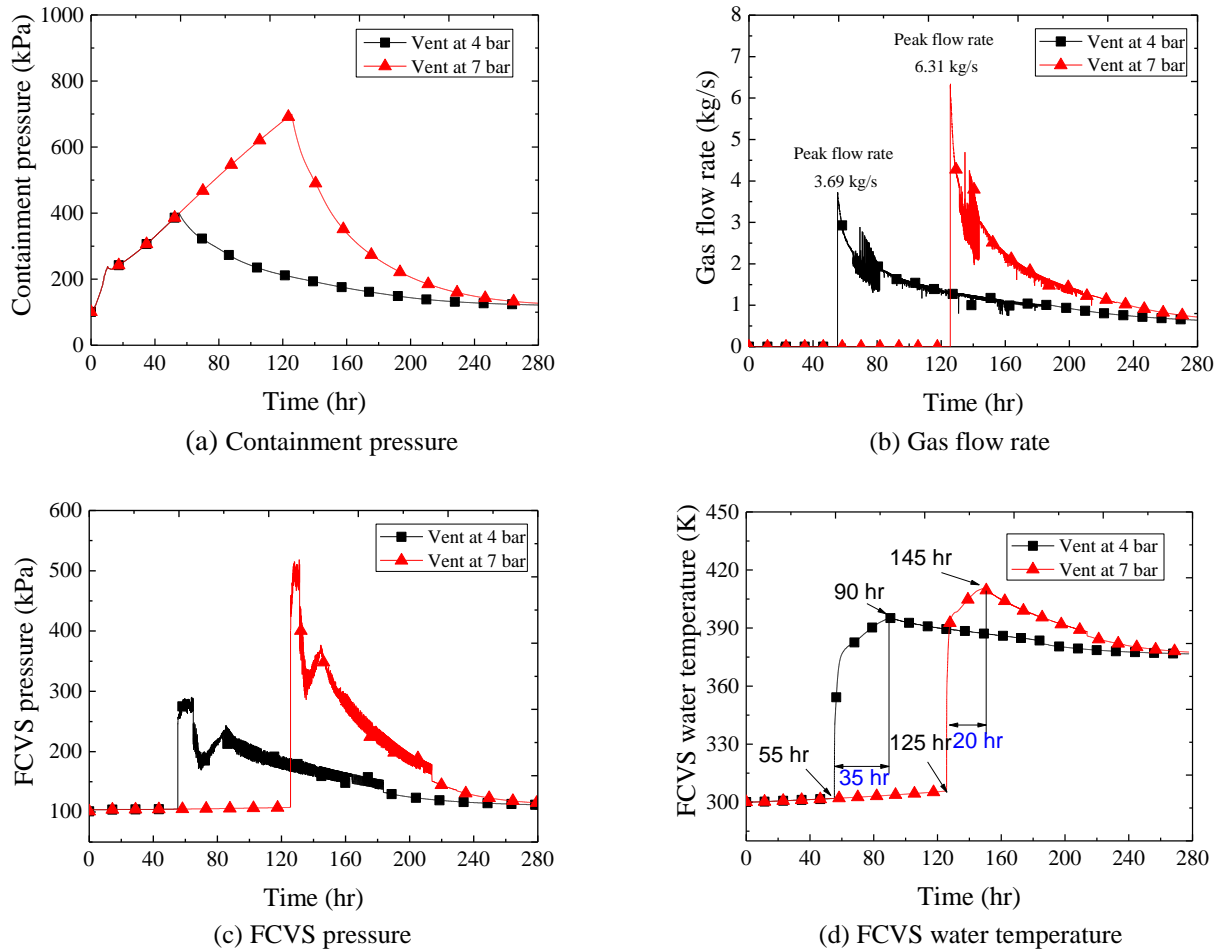


Fig. 7. Effect of vent initiation pressure.

III.A.3 Effect of Vent Initiation Pressure

This section provides the effect of the containment pressure at the time of vent initiation. The cases are P7O10D10DF3 and P4O10D10DF0 in TABLE I where the vent initiation pressure is 7 bar and 4 bar, respectively and the pipe size is 10 cm.

The variations of the containment pressure, the gas flow rate through the FCVS inlet junction, the FCVS pressure and the water temperature are presented Fig. 7. Vent initiation at higher containment pressure means late opening the isolation valves as shown in Fig. 7(a). One major result to be noted from this analysis is that even though the opening is late (vent initiation at higher 7 bar), the absolute time from the accident initiation to reaching 2 bar is almost the same (300 hr) to the vent initiation at 4 bar as shown in Fig. 7(a), even though the duration is shorter for the vent initiation at 7 bar than at 4 bar (175 hrs vs. 250 hrs). This is due to larger discharge flow rate for the case of vent initiation at 7 bar than at 4 bar (peak flow rates 6.31 vs. 3.69 kg/s) as shown in Fig. 7(b). FCVS pressure and temperature are thus higher for the high pressure vent as shown in Figs. 7(c) and (d). The elapsed times to maximum temperatures are 20 hrs vs. 35 hrs, respectively.

Therefore, vent initiation at higher containment pressure may be beneficial for more rapid depressurization whereas the dynamic loading to the FCVS is higher and FCVS water exhausts earlier, which are maleficent.

III.A.4 Effect of Isolation Valve Stroke Time

To evaluate the influence of isolation valve stroke time, analysis is conducted for isolation valve stroke times of 10 sec (P4O10D10DF0) and 60 sec (P4O60D10DF3 in TABLE I). The stroke time has completely negligible effect on the depressurization of the containment as shown in Fig. 8. Nevertheless, under practical situation, it can be stated that slow opening is much more beneficial to reduce dynamic pressure loading on the piping and the FCVS tank.

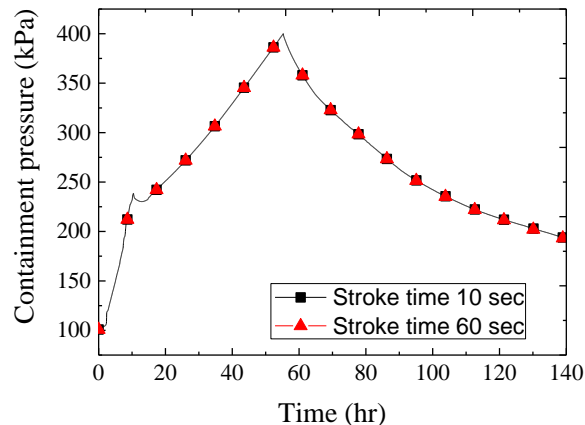


Fig. 8. Effect of stroke time for vent at 4bar.

III.B. FCVS Water Depletion

Based on the analyses above, larger pipe size and higher vent pressure would result in large discharge gas flow rates. The larger the gas flow rate is, the shorter the elapsed time to saturation will be. If the FCVS water reaches saturation earlier, the steam condensation will be degraded and this would increase the uncondensed steam flow to the upper region and resulting aerosol release to the environment will be increased. Furthermore, if the FCVS water depletion is accelerated, the operator should refill the FCVS after closing the isolation valves to maintain proper operation. However, this would be disturbing overall severe accident management and increase the operator stress. Therefore, alarming of early water depletion according to pipe size and vent initiation pressure will be useful for the operator and the elapsed time to saturation can be as good an indicator of the FCVS water depletion as the core exit temperature in a reactor vessel used as an indicator for the reactor core uncover.

Therefore, effects of vent initiation pressure and pipe size on the time to FCVS water saturation are analyzed for several combinations of the two parameters said and the results are presented in Fig. 9. The vent initiation pressure ranges from 4 to 7 bar and the pipe size ranges from 10 to 20 cm. The elapsed time to saturation according to the pipe size is significant, e.g., for the vent initiation at 4 bar. The saturation time is 35 hrs for the 10 cm pipe whereas 12 hrs for the 20 cm pipe as shown in Fig. 9(a). The values are three fold. On the other hand, the effect of vent initiation pressure for given pipe size is not so high and almost negligible for larger pipe size, 20 cm.

Figure 9(b) shows the water depletion according to elapsed time (from the vent initiation) for the extreme pipe sizes, 10 cm and 20 cm. The resulting depletion times are 113 hrs and 21.5 hrs (5.3 fold), respectively. The ratio is comparable to that of the saturation times (3 fold) shown in Fig. 9(a). This shows that the elapsed time to saturation can be a good indicator of the time to FCVS water depletion.

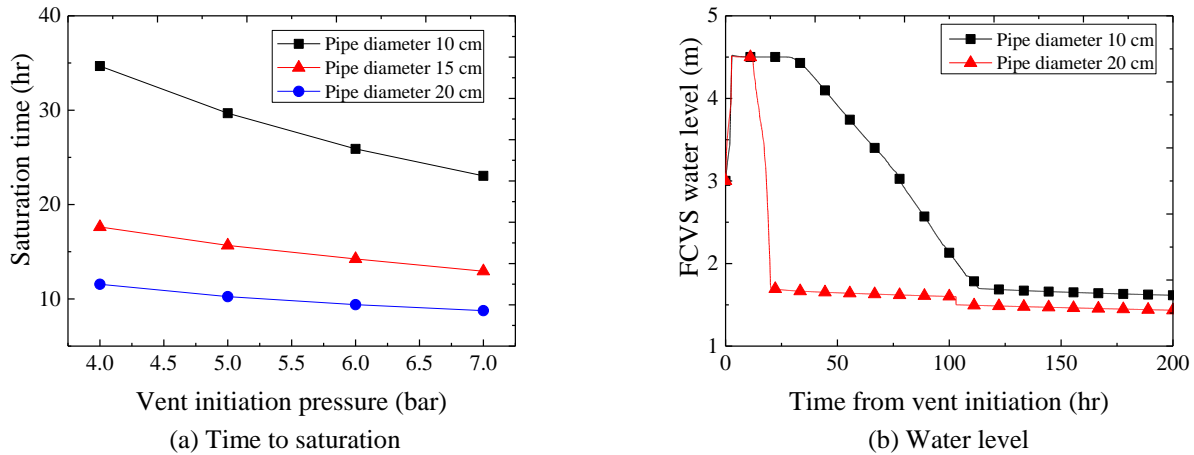


Fig. 9. Elapsed time to saturation and water depletion in the FCVS.

III.C. Fission Product Release Amount

Figures 10 shows the CsI release into the environment for the case of vent at 4 bar through a 10 cm pipe (P4O10D10DF0). The effect of complete water depletion in the FCVS on the CsI release mass is shown in Fig. 10(a) and the mass for the dry FCVS is about 100 times larger than the wet condition. This is because we assumed constant aerosol DF value of 100 for the FCVS water pool and this confirms the decontamination calculation is properly conducted. Figure 10 (b) shows the CsI mass released for the conditions in TABLE I except for the last one (P4O60D10DF3), which is excluded since the result is not different from the second case (P4O10D10DF0). For the uncontrolled failure case (P8D20FAIL) in Fig. 10(b), the break hole diameter assumed is 20 cm.

Figure 10(b) shows that the CsI releases for almost the filtered venting cases are less than the uncontrolled failure at 8 bar with a break hole diameter of 20 cm. However, there is an exception: the case of same diameter pipe (20 cm) and low pressure vent at 4 bar (P4O10D20DF3 in TABLE I): total CsI mass released is larger than that of the uncontrolled failure (P8D20FAIL). This can be explained as following: For the vent initiation at higher pressure, in-containment gas contains more steam than under lower containment pressure as shown in the Fig. 11(a), and thus the CsI concentration at vent initiation at 4 bar is larger than that of the uncontrolled failure at 8 bar from the 2.5 hr to 7.5 hr as shown in Fig. 11(b). This results in larger mass of CsI per unit volume of effluent from the containment to the FCVS for the case of P4O10D20DF3. Moreover, the CFVS pool water is depleted after about 25hrs for the P4O10D20DF3 case as shown in Fig.9(b) and this results in no decontamination (DF = 0) and further increases the CsI release for this case. This integral effect results in larger cumulated CsI mass released into the environment (areas below the curves in Fig. 11(c)) for the case of vent initiation at 4 bar.

This trend is also observed, as shown in Fig 11(d), for the three uncontrolled containment failures at 7, 8 and 9 bar with the same break hole diameter of 20 cm. The ratio of CsI release mass for the failure at 7 bar is about 10 times larger than the failure at 9 bar.

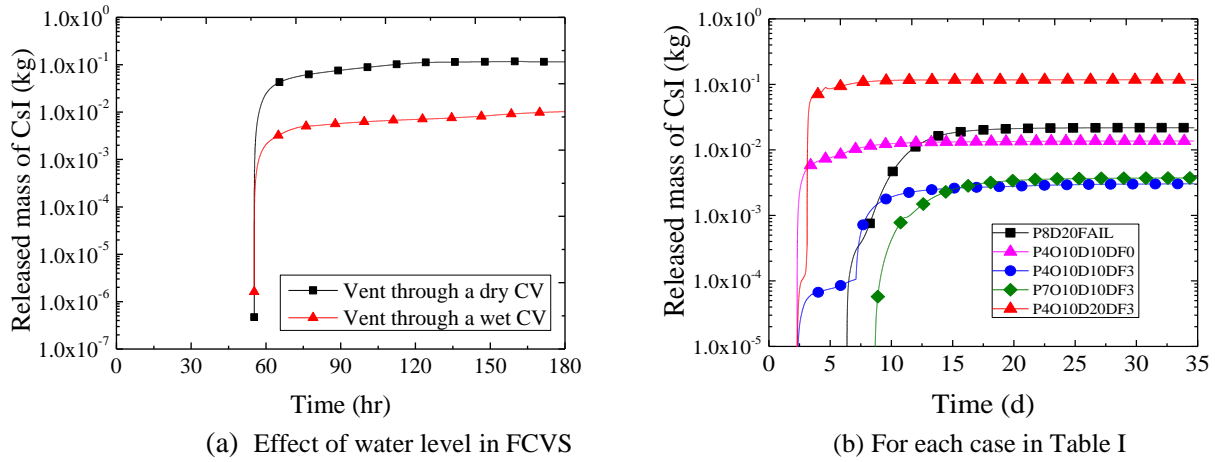


Fig. 10. CsI mass released to environment.

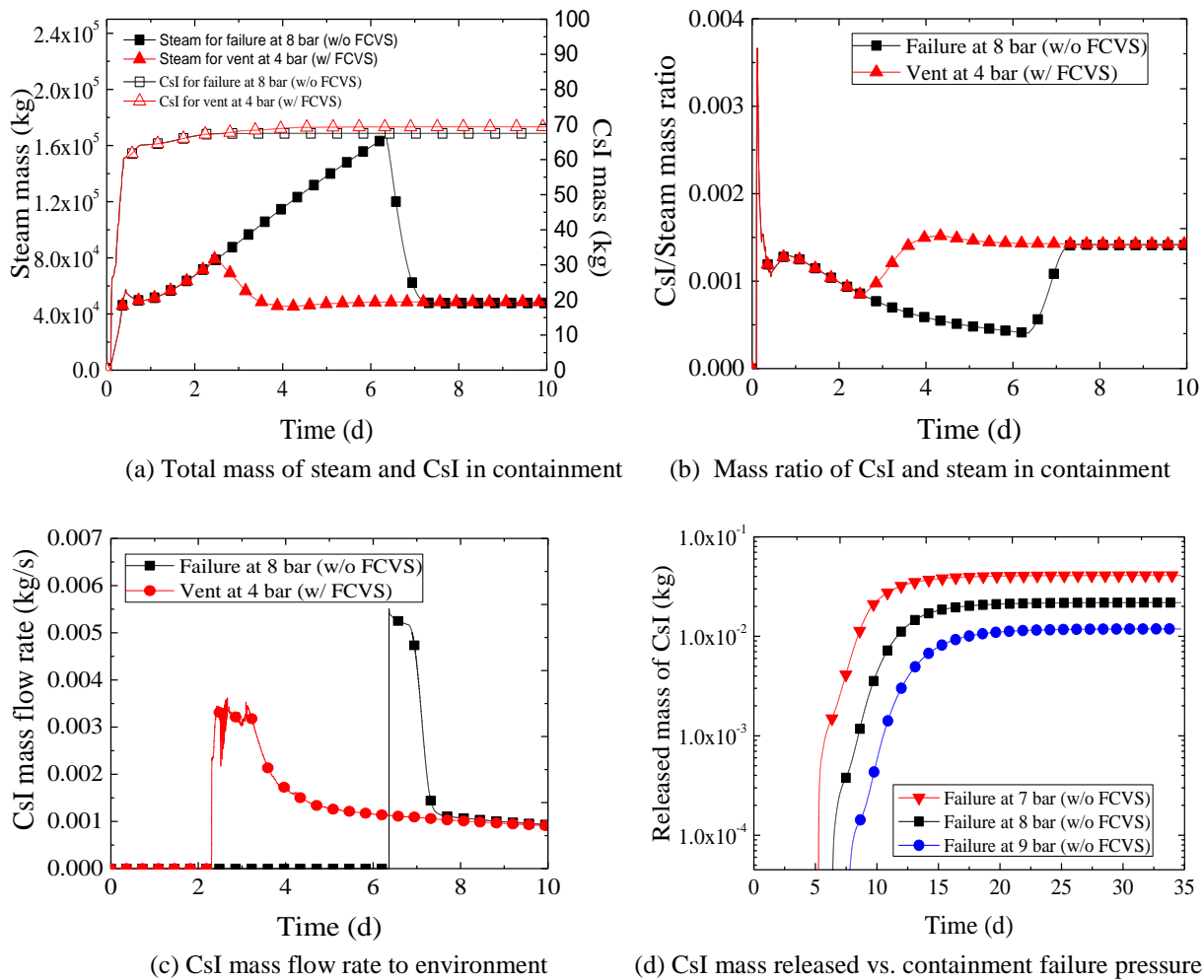


Fig. 11. Effect of vent initiation pressure on release parameters.

On the other hand, for the smaller pipe with 10 cm diameter, the CsI mass release for the filtered venting at 7 bar (P7O10D10DF3) is slightly larger than that for 4 bar (P4O10D10DF3) as shown in Fig. 11(b). This is because, for the 10 cm diameter pipe, the effect of in-containment CsI concentration according to pressure vanishes due to lower discharge flow rate than for 20 cm pipe.

The results above come from the assumption of conservatively low FCVS DF of 100, which considers degraded FCVS condition. Therefore, further study is required for larger DFs by modeling venturi scrubber's aerosol removal whose DF is known to be larger than 1000 (Ref. 2).

IV. CONCLUSIONS

As standpoints of risk and performance, effects of FCVS design and operational parameters on the containment depressurization, FCVS degradation and CsI release are analyzed for the APR1400 using the MAAP4 code. A wet type FCVS is modeled by using a control volume comprising water and gaseous regions connected with an inlet junction from the containment and an outlet junction to the environment. Three types of analyses are conducted: first analysis is to determine the time elapsed for the containment pressure to reach 2 bar after vent initiation at 4 and 7 bar, the pipe sizes of 10 or 20 cm, isolation valve stroke time for 10 and 60 seconds. The analysis result can be summarized as following: irrespective of the vent initiation pressure, the absolute time from the accident initiation to reaching 2 bar is almost the same (300 hr) for 10 cm pipe. In these cases, the water temperature in FCVS depletes earlier for the venting at higher pressure. In the analysis on the effect of the pipe size and the valve stroke time, it is determined that larger pipe size results in more rapid depressurization but there is negligible effect of valve stroke time on the depressurization rate. Therefore, it can be stated that smaller venting pipe size and slow valve opening will be more advantageous in reducing the pipe and FCVS loading. Coupled effects of vent initiation pressure and pipe size on the time to FCVS water saturation are analyzed for several combinations of the two parameters. For the vent initiation pressure ranging from 4 to 7 bar and the pipe size ranging from 10 to 20 cm, the time to saturation according to the pipe size is significant, e.g., three fold. On the other hand, the effect of vent initiation pressure is not so high for given pipe diameter and it is negligible for larger pipe size. The water depletion time ratios are comparable to that of the saturation time ratios and it is thus concluded that the time to saturation can be a good indicator of the time to FCVS water depletion. For the CsI release through large pipe (20 cm) under degraded FCVS filtering performance, the releases for low pressure venting may be larger than for the uncontrolled failure at higher pressure. It is determined that this is because in-containment gas contains less steam at lower pressure than at higher pressure and the CsI concentration tends to increase. This needs further investigation with more sophisticated models. In the future, detailed modeling of the venturi scrubber and pool direct contact condensation is thus required for more realistic estimation of the containment and FCVS performance.

ACKNOWLEDGMENTS

This research was supported partly by a grant from the nuclear safety research program of the Korea Foundation of Nuclear Safety with funding by the Korean Government's Nuclear Safety and Security Commission (Grant Code: 1305008-0416-SB120). and partly by Nuclear Safety Research Program (NRF- 2016M2A8A4903031) of National Research Foundation of Korea (NRF) funded from Ministry of Education, Science & Technology (MEST).

REFERENCES

1. N.R. LEE, Y. S. BANG, T. K. PARK, D. Y. LEE, "Numerical Study of Sever Accidents of Containment Venting Conditions", *ICAPP 2015*, Nice, France, May 03-06, (2015).
2. K. YUAN, D. Q. GUO, L. L. TONG, X. W. CAO, "Evaluation of containment venting strategy via VFS path for advanced passive PWR NPP", *Progress in Nuclear Energy*, **73**, 102 (2014).
3. Y. S. NA, K. S. HA, R. J. PARK, J. H. PARK, S. W. CHO, "Thermal Hydraulic Issues Of Containment Filtered Venting System For A Long Operating Time", *Nuclear Engineering And Technology*, **46**, 6 (2014).
4. PH. DEJARDIN, T. HELMAN, J. BULLE, J. DIENSTBIER, L. OURY, L. SALLUS "Methodology developed for the definition of the design parameters and associated safety criteria of the Filtered Containment Venting Systems", *Progress in Nuclear Energy*, **93**, 58 (2016).

5. USNRC, *Consideration of Additional Requirements for Containment Venting Systems for Boiling Water Reactors with Mark I and Mark II containments*, SECY-12- 0157, Enclosure 5a (2012).
6. NEA/CSNI, *OECD/NEA/CSNI Status Report on Filtered Containment Venting*, NEA/CSNI/R7 (2014).
7. MAAP4 -Modular Accident Analysis Program, Fauske & Associates, inc.
8. A.M. SILVA, J.C.F. TEIXEIRA, S.F.C.F. TEIXEIRA, “Experiments in a large-scale venturi scrubber Part I: Pressure drop”, *Chemical Engineering and Processing*, **48**, 59 (2009).
9. J.W. PARK and W.C. SEOL, “Considerations for severe accident management under extended station blackout condition in nuclear power plant, *Progress in Nuclear Energy*, **88**, 245 (2016).